Journal of Applied Engineering Sciences & Technology Vol. 5 No. 2 (2025) 139

Issues lists available at UMKB journals

Journal of Applied Engineering Sciences & Technology

Journal home page: https://journals.univ-biskra.dz/index.php/jaest

Doi : https://doi.org/10.69717/jaest.v5.i2.139

# Design and Deployment of a Low-Cost IoT-Based Air Quality Monitoring System Using ESP32, BME688, and MQ135 Sensors in Urban Lagos, Nigeria

Ibifubara Humphrey[1,*], Adeyinka David Adewoyin[1], Olamide Florence Humphrey[2], Oluwasegun Timothy Fakorede[1]

[1]*Department of Physics, University of Lagos, Lagos, Nigeria.*
[2]*Department of Biological Science, Mountain Top University, Ogun State, Nigeria*

**ABSTRACT**

This study presented the design, calibration, and in-field deployment of an IoT sensor network at a low cost for monitoring real-time urban air quality in Lagos, Nigeria, for diurnal and locational differences in Carbon-dioxide ($CO_2$), Nitrogen dioxide ($NO_2$), Methane ($CH_4$) and weather parameters. The homemade system, constructed for $83.95, provided multi-gas and weather monitoring at a cost 27–81% lower than mid and high-end commercial sensors. Five hotspots with elevated risk—Oshodi, Iyana-Ipaja, UNILAG dump site, Olusosun, and Super Bus Stop dump site were assessed by morning (06:00–09:00) and evening (19:00–22:00) sessions. Nighttime pollutant levelswere always higher, with $CO_2$ reaching790 ppm compared to740 ppm in morning, and $CH_4$ highest at 0.44 ppm ((Olusosun landfill). These increases were during times of elevated temperature (27.9-32.7 °C), humidity (68–79%) and lower atmospheric pressure (1003–1012 hPa), conditions that would have restricted vertical dispersion. High positive correlations ($r \geq 0.83$, $p < 0.05$) existed between meteorological parameters (atmospheric pressure, relative humidity, and temperature) and the four detected pollutant concentrations (MQ135 index, $NO_2$, $CO_2$, and $CH_4$) during morning and nighttime sampling durations. The system maintained >95% uptime and gave data output within three seconds of data taking, and was therefore highly reliable and robust for tropical urban environments. This method offers an affordable, scalable model of continuous pollution monitoring and evidence-based urban environmental management for rapidly growing cities.

**KEYWORDS**

Low-cost device
Air quality
Meteorology
Diurnal variation
Urban pollution

| ARTICLE HISTORY | Received | Revised | Accepted | Published |
|---|---|---|---|---|
| | 29 Oct 2025 | 01 Dec 2025 | 03 Dec 2025 | 05 Dec 2025 |

## 1 Introduction

Air pollution is a long-standing worldwide environmental problem with extensive effects on ecosystem, public health, and climatic stability. Its relevance has grown more significant, especially in fast urbanizing nations where car emissions and industrialization are on the rise [1]. According to the World Health Organization estimate, air pollution alone is responsible for millions of premature deaths each year and is among the leading causes of cardiovascular and respiratory diseases [2, 3]. In countries such as Nigeria, urbanization may take place without adequate investment in preventing pollution, leaving highly settled cities such as Lagos State vulnerable to toxic air pollutants such as carbon dioxide ($CO_2$), nitrogen oxides ($NO_x$), methane ($CH_4$), ammonia ($NH_3$), and volatile organic compounds (VOCs) [4, 5]. The pollutants pose grave health risks as well as hasten environmental degradation and climate change.

Good air quality monitoring is needed for effective environmental regulation and public health protection. The conventional networks, though, use fixed, complex, and costly equipment, and thus it is only possible to install them in a limited number of urban locations [6]. The peri-urban and poor communities are thus usually out of sight in real-time monitoring, resulting in big spatial and temporal pollution gaps [7]. These blind spots impede responsive policymaking, particularly where pollution is caused by localized activity such as open burning of wastes, industrial effluent discharge, and traffic congestion.

The latest development in Internet of Things (IoT) and embedded system technology has provided air quality monitoring with the portability and accessibility it needs. Environmental sensors such as the BME688 and MQ135 have been coupled with microcontrollers such as Arduino and ESP32 to provide real-time wireless data acquisition systems [8, 9]. Bosch Sensortec's BME688 offers all-time simultaneous measurements of humidity, pressure, temperature, and gas concentration with integrated AI for better gas detection. MQ135 is commonly used for pollutants like $CO_2$, $NO_x$, $NH_3$, benzene, and smoke, and it is for general-purpose use in air quality [10].

Despite all these technological breakthroughs, there is a lot of work in current literature that occurs almost solely in western and Asian countries, and hardly any has been tailor-made to fit the particular environmental and infrastructural characteristics of African

* Corresponding author. Ibifubara Humphrey *(I. Humphrey)*
*E-mail :* ihumphrey@unilag.edu.ng

cities [11]. In the Lagos State scenario, there continues to be a shortage and disaggregation of real-time air quality data. Most available studies highlighted laboratory calibration or small-scale pilot deployments, commonly with weak field robustness.

This research bridged this gap by developing, implementing, and deploying low-cost IoT air quality monitoring using the ESP32 microcontroller, BME688, and MQ135 sensors. ESP32 offers dual-core processing capabilities, Wi-Fi/Bluetooth features, and support for real-time cloud communication. The system is targeted at measuring crucial atmospheric parameters and pollutant concentrations, wireless data transmission to platforms like ThingSpeak or Firebase, and real-time visualization and alarms.

The objectives of this work included designing, integrating, and tuning low-cost IoT-based sensors at an optimal performance for monitoring high-priority urban air pollutants. This included developing proprietary firmware to enable efficient data collection and wireless communication between nodes. The system was installed strategically at the high-risk pollution hotspots around Oshodi, Iyana Ipaja, UNILAG, Olusosun, and Super Bus Stop dumpsites in Lagos State to record spatial and diurnal variation in $CO_2$, $NO_2$ and $CH_4$, and MQ135. In addition, the research will demonstrate the intensive testing of the reliability, sensor sensitivity, and field environmental compatibility of the system under actual out-door field conditions, an economical and scalable solution to current urban air quality monitoring.

The novelty of this research liesin itsapplicationbeing and its commercial orientation. Most current works have been done under controlled conditions or have not been implemented in a developing urban area; this project emphasizes field deployment in Lagos, Nigeria. Also, it showed the potential of low-cost sensor-based systems to successfully monitor urban air quality in difficult conditions. Additionally, the system architecture is scalable and modular and can enable future additions of power harvesting from solar power, GPS location tracking, and mobile alerting.

Overall, this work contributes to the growing literature on low-cost environmental monitoring with an implementable and scalable approach for real-time air quality profiling within the urban developing environment. Besides increasing public access to environmental data, the contribution of this work goes toward evidence-based policy-making; it empowers local communities through a bottom-up approach to choose the locations for green infrastructure and supports overall sustainable urban development. The results of this research will help guide future environmental monitoring activities and encourage the replication of similar systems in other African cities facing similar issues.

# 2 Materials and Methods

## 2.1 Study Design and System Architecture

The research used an experimental approach to prototype and test a low-cost, real-time urban air quality sensor network. The system consisted of three levels that were interconnected: sensing, processing, and communication. The sensing level of the system used MQ135 and BME688 sensors to detect temperature, humidity, pressure, gas resistance, and pollutants like $CO_2$, $NO_2$, $NH_3$, benzene, and smoke. The ESP32 microcontroller was the processor and was used for interfacing with sensors, processing data, and transmitting data. Lastly, data was transmitted to cloud platforms, in this instance ThingSpeak, for remote access, real-time monitoring, and long-term environmental data storage.

## 2.2 Hardware Components

Hardware elements of the system were the ESP32 microcontroller, chosen based on low power, on-chip Wi-Fi, analog and digital communication interface. The microcontroller processed MQ135 analog outputs and interfaced with the BME688 via I²C. The BME688 delivered temperature, humidity, pressure, and gas resistance values with calibration, while the MQ135 sensed pollutant gases following $R_0$ baseline resistance calibration. A 0.96-inch OLED display provided real-time on-site measurement of environmental parameters. Power was drawn from a rechargeable lithium-ion battery using USB, with optimized power consumption achieved via the ESP32 deep sleep mode.

The sensor assembly was subsequently installed in a custom environmental enclosure that limited direct exposure to rain, dust, and radiant heating while allowing for sufficient airflow in order to promote gas diffusion. The enclosure was made up of double-layer weather-resistant plastic shell. Ventilation was provided through side-entry louvered openings with 3-4 mm perforations along the bottom edge of the bee-box for passive cross-ventilation without allowing splash access. The MQ135 and BME688 sensors were fixed inside the enclosure in a clutter-free manner around 20 mm from walls of the box to minimize thermal contamination and ensure that there was no mixture between indoor wind. No active fans were applied, but a natural convection allowed continuous air perfusion at the level of 1-2 L/min, consistent with low-turbulence diffusion chambers recommended for m-o sensor installation. A 120 µm fine mesh filter was installed to minimize particle deposition, and hence long-term drift. The sensors were mounted at about an elevation of 2 m to correspond to mean human exposure rates.

## 2.3 Software Development

Firmware was developed with Arduino IDE and PlatformIO, including large libraries for sensor initialization, data reading, and connecting to the cloud. BSEC library converted raw outputs of the BME688 sensor to calibrated temperature, humidity, pressure, and air quality data. Wi-Fi and HTTP libraries provided reliable internet connectivity and data transfer to ThingSpeak as HTTP POST requests. Environmental readings were taken every minute, and transmission every five minutes was tuned for data resolution versus power efficiency. This was intended to provide consistent real-time measurement, minimize the utilization of power, and enable constant remote access of environmental measurements from cloud-based dashboards.

## 2.4 Cloud Integration and Visualization

Environmental data were sent to ThingSpeak and Firebase, where real-time and historical visualization wereoffered through time-series graphs and AQI indicators on personalized dashboards. Remote accessibility from devices connected to the internet made it an effective feature for real-time monitoring, environmental monitoring, and quick decision-making.

## 2.5 Calibration, Testing and Gas Estimation

The MQ135 gas sensor was calibrated following the manufacturer's recommendations and semiconductor gas-sensor principles outlined in supporting material. In order to stabilize the tin-oxide heating element of the sensor, a 48-hour preheating was performed [12]. Baseline resistance, $R_0$, was determined next under clean-air conditions with the use of the standard Equation 1 and 2:

$$R_s = R_L\left(\frac{V_c}{V_{out}} - 1\right) \tag{1}$$

$$R_o = \frac{R_s}{K_{clean\ air}} \tag{2}$$

where $R_L$ is the load resistance and $K_{\text{clean air}}$ is the clean-air sensitivity factor from the MQ135 datasheet [13].

The MQ135 responds to a wide range of interfering gases; as such, its performance is normally influenced by variations in temperature and humidity, as represented in the datasheets provided [13]. Therefore, the pre-calibrated values must be corrected based on the aforementioned environmental factors for proper sensing [14]. In order to minimize drift resulting from variations in humidity and temperature, the calibrated value $C_v$ was calculated using Equation 3.

$$C_v = \frac{R_S}{R_o} D_{TH} \tag{3}$$

where, $D_{TH}$ represents the temperature and humidity dependence value for calibration.

The MQ135 does not directly quantify individual gases but requires pre-calibration to measure gas capacity, whereby changes in the ratio of $R_s/R_0$ are converted into approximate pollutant-indicator values using empirical relationships derived from published sensor-characterization studies in Equation 4.

$$C_x = a\left(\frac{R_S}{R_0}\right)^b \tag{4}$$

where $C_x$ is an estimated concentration index for $CO_2$, $NO_2$, or $CH_4$, and coefficients a and b are extrapolated from the curves provided in the sensor's data sheet [13-15].

## 2.6 Deployment Strategy

Field measurements were carried out at five of the most contaminated urban locations in Lagos, Nigeria, which are Olusosun, UNILAG Dump Site, Oshodi, Iyana Ipaja, and Super Bus Stop—which were chosen based on their strong emission source and human traffic. The units were mounted outdoors at about 2 m ground level in weather-resistant enclosures to mimic human exposure and reflect actual air quality fluctuations.

## 2.7 Challenges and Mitigation Strategies

Environmental conditions such as temperature and humidity affected MQ135 measurements; live correction was applied on BME688 measurements. Power disconnections were reduced with USB-rechargeable power banks, disconnection handled with buffering measurements on ESP32 until reconnection. Thermal build-up was avoided with ventilated enclosures and mounted in shady areas, ensuring stability of sensors and accurate air quality measurement under fluctuating urban conditions. According to Idrees et al. [16], a measurement that is far from the normal pattern of the measured data is called an outlier. They need to be detected and removed to get correct data. A data smoothing procedure was employed for filtering out this noise. The BME688 gas index was only used qualitatively to indicate the total VOC load and trends in indoor air quality. No conversions were made from the gas index to pollutant-specific concentrations.

### 2.8 Study Area, Data Collection and Analysis

The experiments were carried out at five urban hotspots in Lagos, Nigeria, chosen because of their high traffic volumes, waste disposal practices, and likelihood of having high pollution levels. The study sites are Oshodi (6.53°N, 3.35°E), Iyana Ipaja (6.61°N, 3.30°E), UNILAG dump site (6.52°N, 3.66°E), Olusosun landfill (6.59°N, 3.38°E), and Super Bus Stop (6.64°N, 3.30°E). These consist of a combination of commercial, residential, and waste disposal settings and represent the diverse air pollution conditions of Lagos. Geographical coordinates of the locations were determined using hand-held global positioning system (GPS) units and confirmed by ArcGIS software, which was also used in creating a spatial map of the study area (Figure 1). This allowed for proper referencing of the locations and the visualization of pollutant spatial distribution. Data were recorded at 5-min intervals and automatically averaged hourly. The sampling was conducted between morning (06:00–09:00) and evening (19:00–22:00) sessions to exploit the diurnal behavior influenced by traffic movement, waste burning, and atmospheric stability. These averaging times were selected because they represent typical durations of early morning atmospheric mixing and nights boundary layer stabilisation respectively. Important parameters were temperature, humidity, gas resistance, and pollutant estimation were recorded. Spatial-temporal pollution trends, sensor performance, and environmental correlations were the subject of the analysis with Microsoft Excel and Python libraries (Pandas, Matplotlib, NumPy) used for trend plots, descriptive statistics, and time-series plausibility checks.

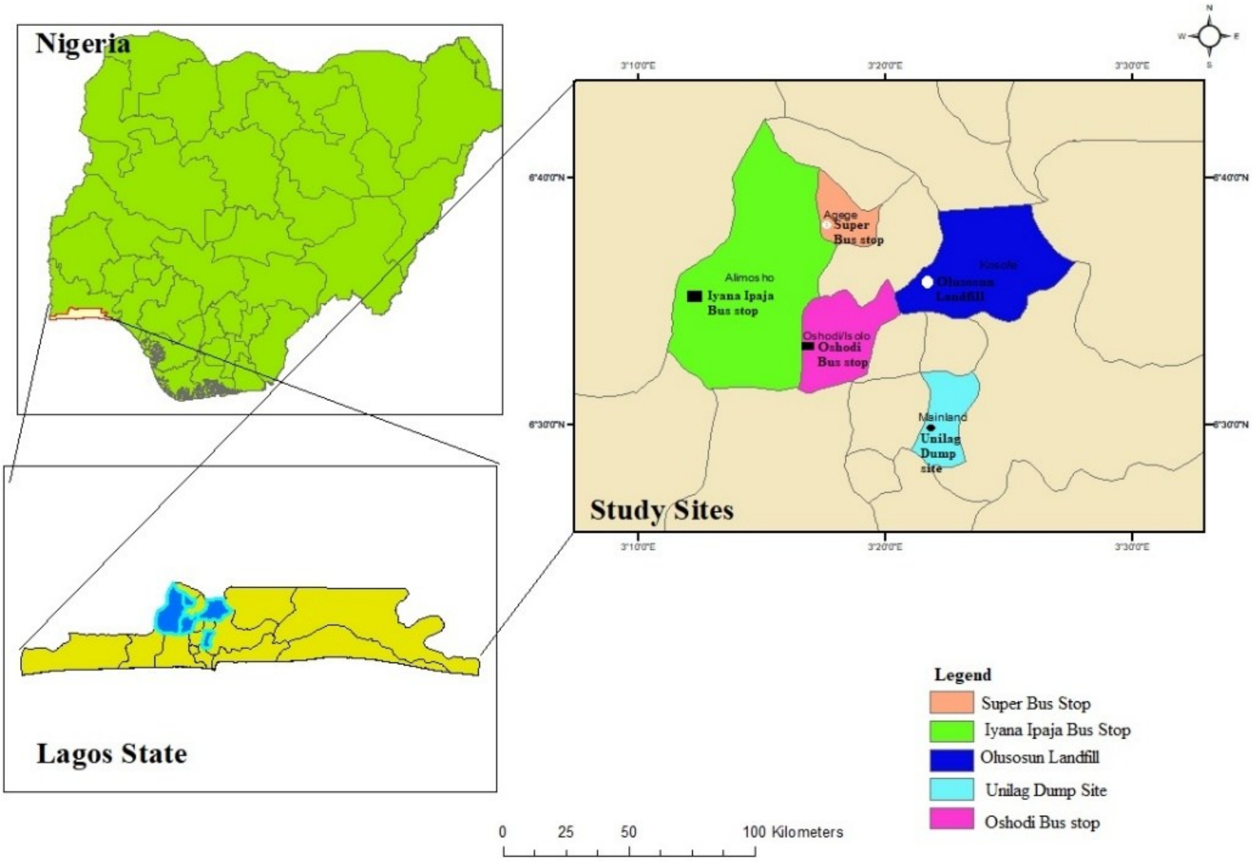


**Fig.1.** Study area and Sampling Location.

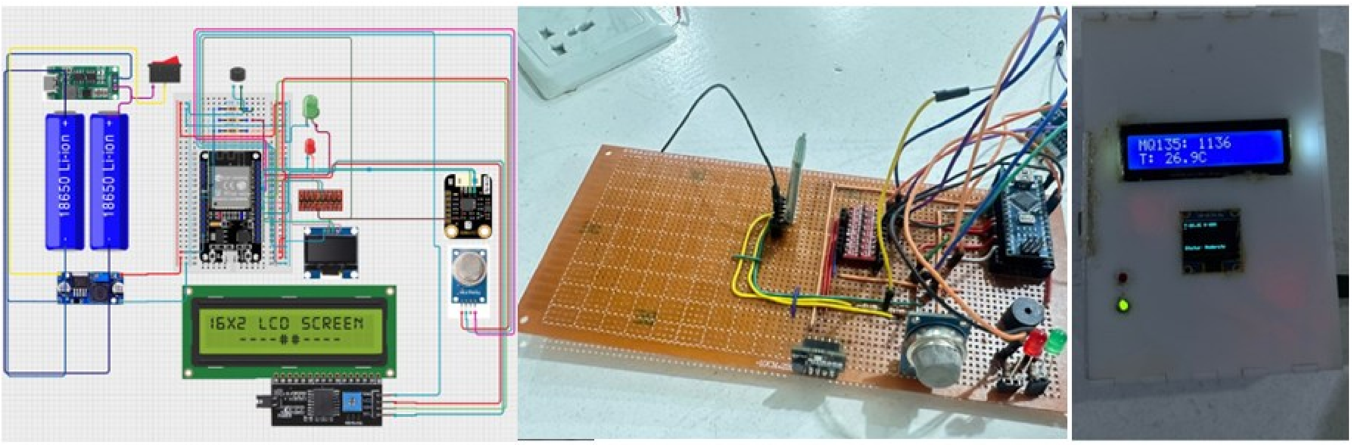


**Fig.2.** A Schematic diagram, Prototype of the Developed Air Quality and Environmental Sensing System.

# 3 Results and Discussion

## 3.1 Developed System Architecture

The system architecture developed was implemented in real-time air quality monitoring successfully, in which multi-parameter sensing capability was embedded in an inexpensive IoT platform. The system provided measurements of key atmospheric parameters like temperature, humidity, and pressure, and key air pollutants such as carbon dioxide ($CO_2$), methane ($CH_4$), and nitrogen dioxide ($NO_2$). The sensor modules were calibrated and connected properly to provide proper, seamless data acquisition and transmission. The computation part integrated into the design provided on-site computing, minimizing latency and maximizing dependability. Data were transferred to a cloud platform for visualization, storage, and analysis, providing remote access and long-term observation of the environment. Robustness under changing environmental conditions was established through performance testing, and stable data and minimal downtime were ensured. These findings demonstrate the system's scalability for deployment in cities with an in-house available, reliable solution for environmental monitoring that serves study, public health policy, and community-based air quality management in resource-poor environments. The prototype air quality and environmental sensing system is depicted (Figure 2).

## 3.2 Cost–Performance Benchmarking of the Custom-Built IoT Air Quality Monitor

The locally developed IoT air quality sensor, costing a total of $83.95, combines exceptional affordability with advanced functionality, performing as good as most market alternatives. Hence, it can be considered an alternative to all the GAIA models, from the high-end GAIA A18 ($322.34 - $437.46) to the low-end GAIA A12 ($115.12 - 230.24), without compromising on comparable multi-gas detection. the GAIA A08 ($57.56 – $115.12) is initially cheaper, matching our system's capabilities requires adding a $CO_2$ sensor (~$48.13), raising its total to $108.46.

Compared to amateur kit like the AirGradient One ($132.31) and Arduino/ESP32 implementations ($24.65), our system combines multi-parameter sensing with weather, features not usually available in such low-cost monitors. This represents a performance-cost ratio of approximately 1.58 times higher than that of the AirGradient One and significantly greater functionality than in amateur Arduino/ESP32 implementations.

Commercial options like PurpleAir (USD 274.99) and AirVisual Pro (USD 406.96) provide trustworthy air quality measurements but are significantly more expensive. Our system, constructed for USD 83.95, achieves multi-gas sensing and monitoring with a high-cost reduction effect. Instead of offering superior performance comparable to commercial products, this system is intended for a cost-effective trend-based monitoring in community implementation for an early warning usage, as well as, spatial coverage extension in low-resource settings. The device offers a repeatable in time and space detection of pollution patterns at a price 27-81% cheaper than mid- and high-end systems, and with functionalities better than low-cost DIY kits. Thus, it is essential to consider the system as a supplementary and low-cost monitoring instrument, but not for a certified reference instrument replacement. A cost performance summary is shown in Table 1.

This combination of expense, sophistication of sensing, and local accessibility makes it an effective, high-impact research tool and community air quality management strategy in resource-scarce settings like Lagos.

**Table 1.** Cost–Performance Benchmarking of the Developed Air Quality Monitoring Device Against Commercial and DIY Alternatives.

| Device | Approx. Cost ($) | Notes |
|---|---|---|
| **Custom IoT System (This Study)** | $83.95 | ESP32 + BME688 + MQ135—modular, low-cost build |
| **Open-Source DIY Kits (e.g., AirGradient)** | $132.31 | Pre-soldered outdoor kit; affordable but single-vendor—source: AirGradient shop (airgradient.com, n.d) [17] |
| **AirVisual Pro (commercial)** | $727.15 | High-precision consumer-grade unit. (https://www.iqair.com, n.d) [18] |
| **PurpleAir Monitor** | $274.93 | Real-time PM2.5/PM10 tracking with strong community support. (https://www2.purpleair.com, n.d) [19] |
| **GAIA A08 + $CO_2$ sensor** | $108.46 | Basic GAIA kit needs external $CO_2$ sensor (https://aqicn.org/gaia/a08/, n.d) [20] |
| **GAIA A12** | $114.62 – $229.24 | Mid-tier model with Wi-Fi and multi-sensor array (https://aqicn.org/gaia/a12/, n.d) [21] |
| **GAIA A18** | $322.38 – $438.07 | Advanced, solar-powered unit with LoRa for off-grid operation. (https://aqicn.org/gaia/a18/, n.d) [22] |

**Table 2.** Geographic Coordinates, Elevation, and Estimated Atmospheric Pressure of the Study Locations.

| Location | Lat (°N) | Long (°E) | Elev. (m) | Est. Pressure (hPa) | Comment |
|---|---|---|---|---|---|
| **Oshodi** | 6.53 | 3.35 | 38 | 1008.6 | Typical coastal pressure |
| **Iyana Ipaja** | 6.61 | 3.30 | 41 | 1008.3 | Slightly higher elevation |
| **UNILAG Dump Site** | 6.52 | 3.66 | 15 | 1011.4 | Closest to sea level – highest pressure |
| **Olusosun Dump Site** | 6.59 | 3.38 | 45 | 1007.9 | Slightly elevated – lowest pressure |
| **Super Bus Stop** | 6.64 | 3.30 | 40 | 1008.4 | Near Iyana Ipaja – similar |

## 3.3 Spatial and Temporal Variations, Implementation Outcomes, and Visualisation-Based Performance Metrics

The analysis showed a diurnal pattern of repeated observations at all the monitoring stations, where the concentrations of pollutants were usually higher at night than in the morning. The night-time predominance was greatest in Olusosun, with $CO_2$ increasing from 740 ppm in the morning to 790 ppm in the night, $NO_2$ from 9.55 ppb to 11.00 ppb, and $CH_4$ from 0.37 ppm to 0.44 ppm. The same trend was observed at the UNILAG Dump Site, with $CO_2$ rising from 670 ppm to 720 ppm—most probably because of decreased vertical dispersion by nocturnal temperature inversions and continuous emissions owing to wastes decomposition. These trends are consistent with earlier Nigerian records of high $CO_2$, $CH_4$, and particulate matter in the early mornings and early evenings due to limited atmospheric mixing [23, 24]. Apart from meteorological factors, nighttime localized activities such as the use of generators and traffic overspill can also increase emissions.

Spatially, Olusosun and the UNILAG Dump Site had the highest loadings and were characterized by active waste decomposition, emission of landfill gas, and little open burning. For Iyana Ipaja and Super Bus Stop, the lowest pollutant loadings were obtained, indicating few emission sources or improved dispersion dynamics. These spatial gradients align with previous Lagos air quality research, in which dumpsite-proximate locations surpassed background urban pollution levels [25, 26], and Olusosun has persistently been shown to surpass WHO air quality standards [23, 27]. Such evidence highlights the necessity of location-specific waste management interventions in dense, tropical cities.

The performance of the MQ135 gas sensor was also highly consistent with expected pollutants trends, ranging from 158 units in Iyana Ipaja (morning) and 275 units in Olusosun (evening). The results were significantly correlated with calculated concentrations, justifying the use of low-cost IoT sensor technology in real-time monitoring (Figure 3). Parallel field deployments in semi-urban Nigeria have also shown MQ135's responsiveness to $CO_2$, $NH_3$, as well as other usual pollutants when used with Arduino-based acquisition platforms [28]. Interwall variability was affected by dumpsite size, waste volume, operating age, and diurnal activity cycles.

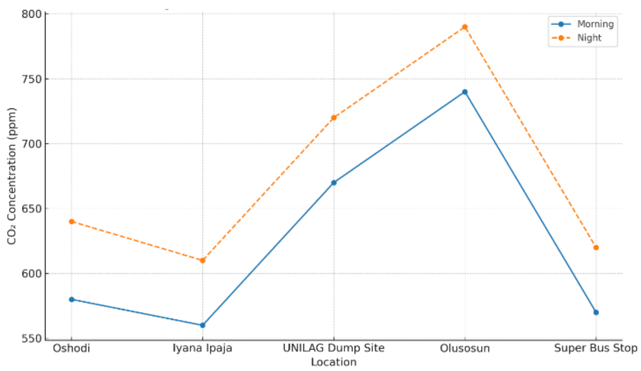


**Fig.3.** Diurnal Variation of $CO_2$ Across Locations.

To best characterize these spatiotemporal dynamics, a blending of various visualisation types was utilized. Bar plots (Figures 4) demonstrated night-time control, and line plots (Figures 3) measured an average ~60 ppm night-time $CO_2$ city-wide rise—characteristic of tropical night-time inversion effects. Heatmaps coupled spatial-temporal dimensions, defining Olusosun and UNILAG as recurring high-intensity areas. Radar plots provided multi-dimensional comparison and depicted Iyana Ipaja and Super Bus Stop as lowest overall but with robust night peaks. Scatter plots revealed statistically significant associations between humidity and all gases monitored and temperature and $CH_4/CO_2$, demonstrating the meteorological sensitivity of pollutant behavior.

The simultaneous line of evidence from pollutant monitoring, meteorological patterns, eye observation, and comparison with literature supports that temporal and spatial trends in Lagos State air quality are strongly moderated by local sources of emissions and atmospheric conditions. Night-time accumulation of pollutants most exemplified at landfill-bordering locations is created through an interaction of compromised dispersion and prolonged emissions. On a public health basis, these mechanisms enhance risk of exposure within nearby communities, especially where residential communities adjoin open dumpsites.

In all, the cost-effective IoT-based network adequately captured spatial and temporal trends, working in accordance with available African urban air quality research. The results invite implementation of interventions in high-pollution hotspots, improved waste management practices, and incorporation of meteorological forecasting in urban pollution control planning.

The relationship between atmospheric pressure and elevation is well-established in atmospheric physics. According to the hydrostatic pressure law ($dP/dh = -\rho g$), pressure decreases with altitude as a result of the reduced weight of the air column above the surface [29]. This demonstrates that barometric pressure not merely physical height is the primary environmental factor influencing conditions at different elevations [30]. Studies across Nigeria further confirmed that variations in atmospheric pressure are mainly influenced by elevation rather than latitude or longitude (Table 2). Segun et al. [31] observed that radio refractivity patterns, which depend on pressure, temperature, and humidity, vary systematically across the country's climatic zones, reinforcing the altitude-dependence of pressure variation. In this study, the locations—UNILAG (6.52°N, 3.66°E), Olusosun (6.59°N, 3.38°E), Iyana Ipaja (6.61°N, 3.30°E), Oshodi (6.53°N, 3.35°E), and Super Bus Stop (6.64°N, 3.30°E)—fall within a narrow geographic range. Hence, differences in pressure arise predominantly from variations in elevation. The barometric formula, ($P = P_0 e^{(-Mgh/RT)}$), links pressure to altitude and temperature, explaining why the lower-lying UNILAG site recorded the highest pressure (1012 hPa at morning and 1008 hPa at night), while the higher Olusosun site exhibited the lowest pressure (1006 hPa at morning and 1003 hPa at night).

### 3.4 Multi-Parameter Comparisons

Radar and Heatmaps plots were used to compare directly a number of variables at one time between locations. These indicated that Olusosun always had the highest values for all the pollution parameters and meteorological extremes, indicating it to have a massive environmental impact. Iyana Ipaja had the lowest pollutant levels, indicating relatively better air quality.

The radar chart displayed diel and spatial temperature, humidity, pressure, and pollutant (MQ135, $CO_2$, $NO_2$, $CH_4$) patterns across five urban locations in Lagos, Nigeria. The levels of pollutants were highest at night, especially at Olusosun and the UNILAG Dump Site, which was most likely caused by lower atmospheric dispersion, thermal inversion, and steady waste emission. Olusosun (Night) had the highest normalized values, justifying landfills as significant areas of pollution. In contrast, Super Bus Stop and Iyana Ipaja exhibited lower morning concentrations, indicating improved ventilation or more remote sources (Figure 5).

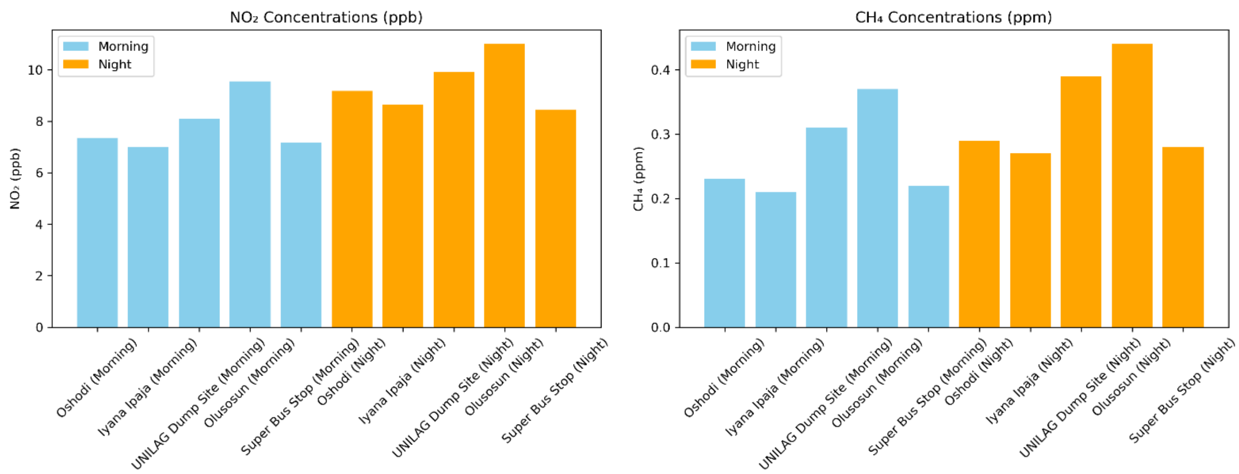


**Fig.4.** $NO_2$ and $CH_4$ Levels by Location and Time.

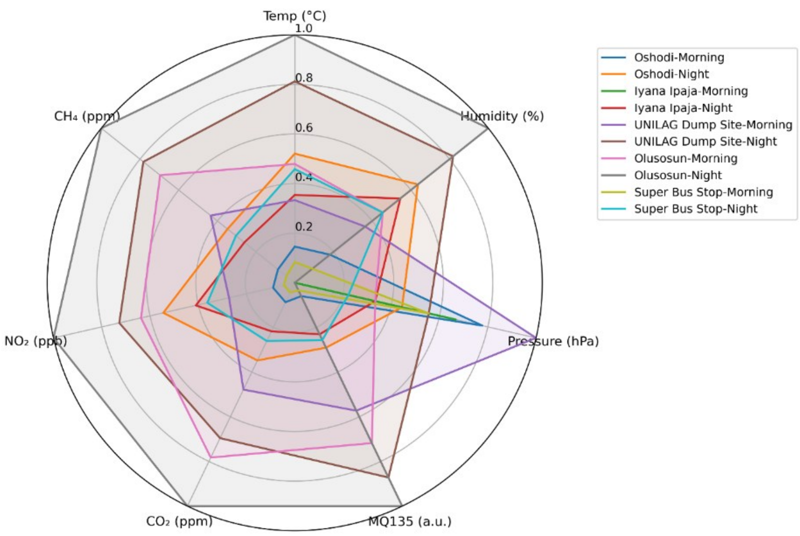


**Fig.5.** Radar plot of normalized environmental and pollutant levels across urban locations in Lagos (Morning vs Night).

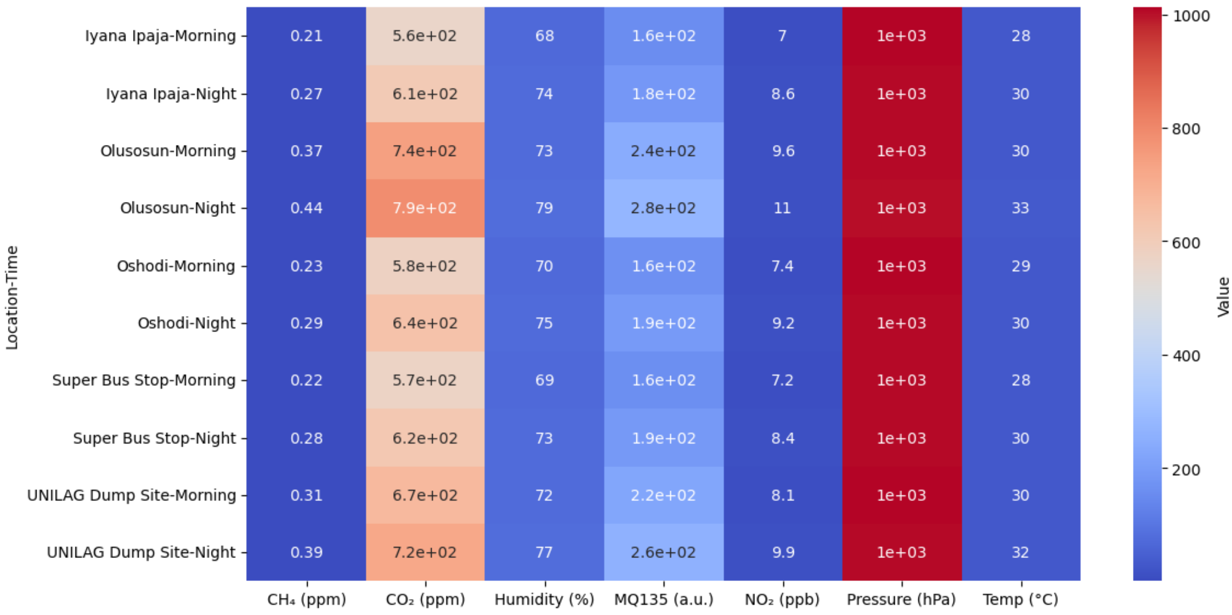


**Fig.6.** Heatmap showing the variation in pollutant concentrations ($CH_4$, $CO_2$, $NO_2$, MQ135) and environmental parameters (Temperature, Humidity, Pressure) across five urban locations in Lagos, Nigeria, during morning and night. Higher values are indicated in warmer colors. $CO_2$ and MQ135 exhibited the highest variation across sites and time.

They reflect findings of high nighttime and dry-season pollutant concentrations downwind of dumps [32], intense temperature–emission relationships for $CH_4$ and $CO_2$ [24]. Meteorological fluctuations—increasing nighttime temperatures and reduced pressure contribute to pollutant accumulation, typical of the diurnal cycle of the atmospheric boundary layer [33]. Stable nighttime atmospheres suppress dispersion, as seen in Po Valley [34].

Similar studies in Iraq, India, and university campuses across the world revealed similar traffic- and landfill-related peaks [35-37]. The findings justified constant, particularly nocturnal monitoring, combined pollutant–meteorology study, and focused interventions in at-risk areas. Improvement in waste management, minimizing open burning, and health education campaigns are essential in minimizing health and environmental effects in the tropics of urban environments.

In addition, the heatmap indicated spatial and temporal changes in pollutant and meteorological parameters at urban sites. Olusosun and UNILAG Dump Site had the highest concentrations of $CO_2$, $NO_2$, and $CH_4$, especially during night hours, and were centers of pollution hotspots. Night concentrations were generally higher as a result of decreased atmospheric dispersion under temperature inversion as well as low wind. At night, temperature and humidity rise, as well as pressure slightly decrease, both of which contribute to pollutant retention. Readings from MQ135 sensors support these patterns, reflecting poorer air quality in polluted areas (Figure 6).

Nigerian urban studies consistently allocate dumpsites and slum settlements as major emission sources, with enhanced concentrations of pollutants during the dry season [32]. Meteorological conditions exhibit strong correlations with emissions [24, 27]. Temperature, microbial activity, and combustion are significant drivers of emissions. Most recent sensor technologies, including Arduino boards derived from MQ135, BMP180, and DHT11 [38-40], and gradient-sensing nodes [41], allow in-situ pollutant and meteorological measurements, lending rigor to data for interventions. The results underscore site-specific regulation of air quality, waste management schemes by zone, and policy interventions to mitigate health and climate risks in tropical cities.

### *3.5 Relationship Between Meteorological Parameters and Pollutant Concentrations*

Scatter plots in Figures 7a–c show three meteorological factors—temperature, relative humidity, and pressure and the four monitored pollutant concentrations ($CO_2$, $NO_2$, $CH_4$, and MQ135 index) for morning and night sampling. Blue represents morning data, and red represents night data, and it is easy to notice differences in daytime. In every site, nocturnal hours were more humid, hotter, and linked to slightly lesser atmospheric pressure than morning. Increases in midday to evening temperatures varied between 27.9 °C (Iyana Ipaja Bus Stop) and 32.7 °C (UNILAG Dump Site), reflecting the persistence of urban heat throughout the night. Overnight, humidity also increased by 68–79%, possibly due to diminished solar heating and enhanced moisture retention in the boundary layer. The minor but recurrent pressure decline (1003-1012 hPa) during the daytime shift may be an indication of local convection initiation activity or air mass stability changes. Between locations, Olusosun and UNILAG Dump Site had the highest temperature and humidity, perhaps because waste decomposition retained heat and released moisture. The site- and diurnal-scale trends indicate that microclimates and anthropogenic activities affect meteorological conditions, which could potentially lead to pollutant dispersion and accumulation in the urban air. The continued reduction of night-time temperatures suppressed the convective mixing, which permitted accumulation of the pollutants. Omokpariola et al. [24] reaffirm previous Lagos-centric findings on the tight temperature–humidity–pollutant relations, particularly relating to $CO_2$ and $CH_4$. Aged landfills-Earlier dumps such as Olusosun emitted more $CO_2$ and methane due to further degradation of waste [23].

Temperature showed very high significant, positive correlation ($p < 0.01$) with all the air pollutants, particularly $CH_4$ ($r = 0.96$) and MQ135 index ($r = 0.90$), whose correlation was very much higher in morning ($CH_4$: $r = 0.97$; MQ135: $r = 0.94$) and night ($CH_4$: $r = 0.97$; MQ135: $r = 0.96$). $NO_2$ ($r = 0.96$) and $CO_2$ ($r = 0.96$) were also very highly correlated during daytime, but much more strongly at night ($NO_2$: $r = 0.95$; $CO_2$: $r = 0.97$) as evident from Figure 7a. At higher night-time temperatures, through the urban heat island, vertical mixing is controlled and pollutant accumulation is allowed; weaker morning effects indicate dispersion by diurnal warming. These findings are aligned with other studies that have reported strong temperature–pollutant associations in urban regions, including those sustained across metropolitan cities with reduced emissions [42]. Urban heat island indicators are well correlated with CO, $NO_2$, and $O_3$ [37], and season maxima of all air pollutants are in winter, save for O3 during summer [43, 44].

Humidity had uniformly high positive correlations ($p < 0.05$) with all the pollutants. NO2 had the highest correlation overall ($r = 0.94$), peaking at night ($r = 0.96$, $p = 0.001$). MQ135 and $CO_2$ had comparable overall correlations ($r = 0.83$), which rose in the morning ($r = 0.96$) and to $r = 0.97$ for $CO_2$ at night. $CH_4$ was likewise highly correlated ($r = 0.88$), with high morning and evening values ($r = 0.96$). These trends imply that high nighttime humidity limits nighttime vertical mixing and facilitates pollutant persistence (Figure 7b). Comparable trends have been seen elsewhere: in Shanghai, $CO_2$ and $CH_4$ followed closely behind humidity [45], and Chinese megacity studies proved location-dependent humidity–pollutant correlations [44]. In Addis Ababa, moderate correlation of NOx with humidity was noted [46]. Overall, humidity has an important role in pollutant dynamics, impacting formation, dispersion, and persistence, highlighting its significance for air quality forecasting and monitoring.

Atmospheric pressure showed very strong positive associations with all pollutants, with the strength of the significance varying by hour. $CH_4$ showed the best global correlation ($r = 0.92$, $p < 0.001$) with always significant p (≈0.03). For both morning and evening categories, the correlation with $CO_2$ was significant for MQ135 ($r = 0.90$, $p < 0.001$) and $NO_2$ ($r = 0.88$, $p < 0.001$) were significantly correlated in the morning and evening. We also found that, even though $CO_2$ had high overall correlation ($r = 0.90$) as opposed to other variables tested, it did not exhibit any diurnal significance. This is in line with increased pressure, which is liable to increase the concentration of pollutants but reduce vertical mixing under stable, high-pressure conditions (Figure 7c). Similar positive trends have been reported [47], although some studies observed weaker detrimental trends with local effects. Cointegrated long-term records of $CO_2$ and $CH_4$ growth rates are confirmed by pressure effects controlled for other meteorological variables [48].

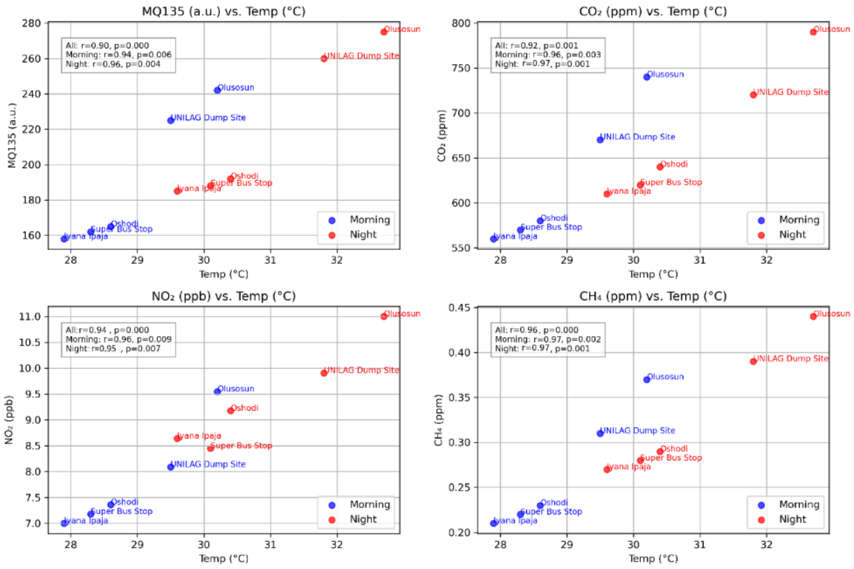


**Fig.7(a).** Scatter plots showing the relationship between temperature and pollutant concentrations (morning in blue, night in red).

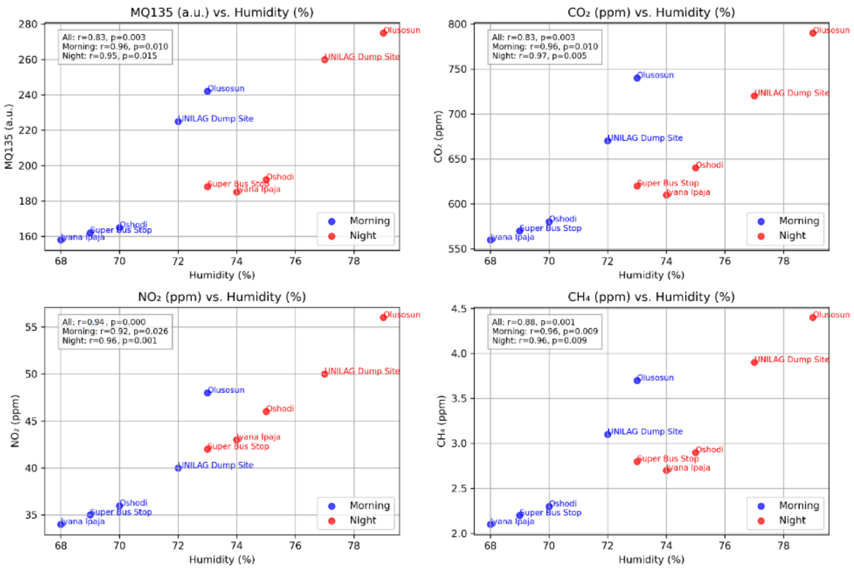


**Fig.7(b).** Scatter plots showing the relationship between relative humidity and pollutant concentrations (morning in blue, night in red).

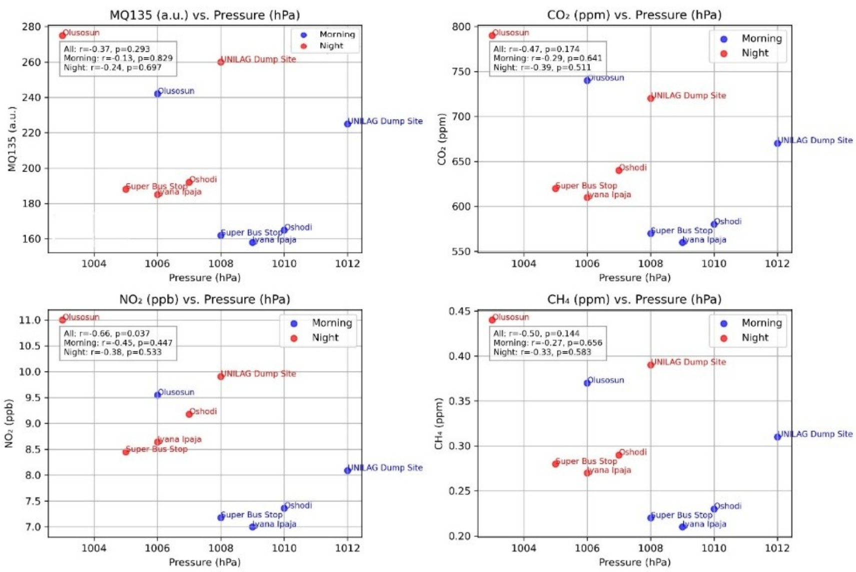


**Fig.7(c).** Scatter plots showing the relationship between relative humidity and pollutant concentrations (morning in blue, night in red).

In general, temperature, humidity and pressure were all positively correlated with pollutant concentrations which was significant at $p < 0.05$ for most of the cases. Conversely, increasing temperature and humidity led to higher MQ135, $NO_2$, $CO_2$, and $CH_4$ concentrations; although the relationship was not uniform across all sensors. $CH_4$ was the greatest and most general correlated one for all parameters. Nocturnal variation was similar, $CO_2$ -pressure relationships were not diurnally significant in predicting short-term variability.

Wind speed also varies inversely with pollutant levels and has different trends relative to other meteorological factors [44, 47]. Ozone rises separately with temperature but reduces with other pollutants, and there are different seasonal trends—most pollutants have their highest levels in winter and ozone during summer [49]. Even though each meteorological effect is small individually, when collectively aggregated, they are very influential in air quality [50], and thereby contribute significantly to air pollution prediction through integration of weather data.

Air quality observations in Lagos State generally register characteristic diel cycles: early morning peaks in $CO_2$, midday maxima in $O_3$; and evening increases in NO, $NO_2$ and CO [51]. Though commercial instruments, such as Aeroqual, employ high-precision NDIR and electrochemical sensors [52, 53], the calibrated MQ135–BME688 platform faithfully reproduced these temporal and spatial patterns. This performance agrees with that of long-term validations suggesting that low-cost sensors capture pollutant trends well although they often lack specificity to individual gases such as $NO_2$ [54]. Large-scale studies, including QUANT [55], further reveal that low-cost systems exhibit variability forced by meteorology - a finding echoed in assessments of unit-to-unit differences and environmental dependence [56]. Yet, multipollutant platforms have reported strong correlations ($r = 0.66 – 0.98$) with reference instruments [57], and performance of $CO_2$ sensors alone improves substantially following calibration [58].

Morning conditions within our dataset were indicative of lower pollutant indicators at 30.10 °C and 73.46% RH, respectively. Correspondingly higher $CO_2$, $NO_2$, and $CH_4$ were measured at night due to suppressed boundary-layer mixing. These patterns are in line with commercial observations and previous low-cost sensor evaluations, supporting the suitability of the system for detecting relative trends and not for regulatory compliance.

Comparisons with commercial monitors were done with caution, recognizing the disparities in sensing technologies. Aeroqual and their variants represent systems based on gas-phase measurements, while the vast majority of low-cost commercial devices such as PurpleAir and AirVisual target particulates via optical scattering. Comparisons focused on temporal and spatial behaviors rather than pollutant-specific accuracy to make fair comparisons across very distinct measurement principles and pollutant classes.

Future studies will consider targeting sensor accuracy, long-term stability, and pollutant specificity. The inclusion of additional reference-grade modules with NDIR sensors for $CO_2$ and electrochemical sensors for $NO_2$/CO would increase the quantitative reliability of the sensors and allow for calibration against certified standards. Machine learning-based calibration models and drift compensation and data fusion from multiple sensors will be explored for improved pollutant discrimination and removal of cross-sensitivity introduced by low-cost semiconductor sensors. Incorporation of particulate matter sensing ($PM_{2.5}$/$PM_{10}$ concentrations) and GPS-derived geolocation would enable the development of more complete urban exposure maps. Subsequent prototypes will also focus on solar powering, miniaturization, and banding of the enclosure to withstand prolonged deployment in tropical environments. Application to denser observation networks will enable spatial interpolation, hotspot detection, and better quantification of microenvironment variation. The analytics performed on the cloud and its user-facing dashboards will be expanded toward community engagement, early warning systems, and real-time public health decision-making.

## 4 Conclusion

The research was able to design and implement a low-cost IoT-based sensor network to monitor urban air quality in real-time in Lagos, Nigeria, for diurnal and spatial variation in $CO_2$, $NO_2$, $CH_4$, and MQ135-sensed pollutants.

The system exhibited satisfactory operational reliability, data transmission at high speed, and flexibility under severe tropical environmental conditions. The results indicated that concentrations of pollutants were generally higher at night and that high humidity and low atmospheric pressure facilitated less vertical dispersion and pollutant concentration. The strong positive relationships between meteorological parameters particularly humidity and pollutant concentrations accentuated the prevailing influence of weather conditions in regulating air quality dynamics. Spatial analysis revealed Olusosun landfill and UNILAG dump site as persisting hotspots of pollution, hence necessitating pre-emptive mitigation measures in waste management sites. Integrating meteorological conditions with real-time measurements of pollutants was crucial for correct appraisal and forecast, enhancing improved environmental planning.

Overall, the study showed the cost-effectiveness and utility of low-cost IoT-based monitoring systems for real-time site-specific air pollution monitoring in resource-constrained environments. The methodology presented a replicable model for other quickly urbanizing cities facing similar air quality issues, supporting evidence-based decision-making towards public health protection and sustainable urban management.

## Disclosure of interests

There is no competing interest.

## Availability of data and material

Data used are reported in the manuscript.

## Authors Contributions

**Ibifubara Humphrey**: The conception and design, analysis and interpretation of the data; the drafting of the paper, revising it critically for intellectual content; and the final approval of the version to be published.

**Adeyinka David Adewoyin:** Investigation, revising it critically for intellectual content, and the final approval of the version to be published.

**Olamide Florence Humphrey:** Analysis and interpretation of the data revising it critically for intellectual content, and the final approval of the version to be published.

**Oluwasegun Timothy Fakorede:** The conception and design, draft preparation, Data curation.

## References

[1] Shaddick, G., Thomas, M. L., Mudu, P., Ruggeri, G., and Gumy, S. Half the world's population are exposed to increasing air pollution. *NPJ Climate and Atmospheric Science. 2020*, *3*(1), 23. https://doi.org/10.1038/s41612-020-0124-2.

[2] Gul, H., and Das, B. K. The impacts of air pollution on human health and well-being: A comprehensive review. *Journal of Environmental Impact and Management Policy*, 2023, *36*, 1-11. https://doi.org/10.55529/jeimp.36.1.11.

[3] Milibari, A. A., Badri, H. M., Khan, W. A., and Rumchev, K. Public perception and knowledge on air pollution and its health effects in Makkah, Saudi Arabia. *Journal of the Air & Waste Management Association*. 2025, *75*(8), 670–681. https://doi.org/10.1080/10962247.2025.2517779

[4] Cordell, R.L., Panchal, R., Bernard, E., Gatari, M., Waiguru, E., Ng'ang'a, M., Nyang'aya, J., Ogot, M., Wilde, M.J., Wyche, K.P. and Abayomi, A.A. Volatile organic compound composition of urban air in Nairobi, Kenya and Lagos, Nigeria. *Atmosphere*. 2021, *12*(10), p.1329. https://doi.org/10.3390/atmos12101329.

[5] Odu-Onikosi, A., Herckes, P., Fraser, M., Hopke, P., Ondov, J., Solomon, P. A., ... and Hidy, G. M.. Tropical air chemistry in Lagos, Nigeria. *Atmosphere*. 2022, *13*(7), 1059. https://doi.org/10.3390/atmos13071059.

[6] Tshuma, M. T., Mckenzie, R., Mathaha, T., Mayana, L., Cervello, A., Chabalala, V., ... and Mellado, B. AI_r: Transforming Air Quality Monitoring through Cost-Effective AI Solutions. In *2024 8th International Artificial Intelligence and Data Processing Symposium (IDAP). 2024,* (pp. 1-8). IEEE. https://doi.org/10.1109/IDAP64064.2024.10710650.

[7] Salsabila, T., Mokoginta, D. P. A., Bonde, G. J. I., Nubala, A. A., Pambela, G. W., Mokoginta, Z., and Al Syarqiyah, S. Low Cost Sensor Technology Innovation in Air Quality Monitoring: A Systematic Literature Review on Opportunities for Public Budget Efficiency. *Journal of Computation Physics and Earth Science (JoCPES).* 2025, *5*(1). https://doi.org/10.63581/jocpes.v5i1.14.

[8] Paithankar, D. N., Pabale, A. R., Kolhe, R. V., William, P., and Yawalkar, P. M.. Framework for implementing air quality monitoring system using LPWA-based IoT technique. *Measurement: Sensors.* 2023, *26*, 100709. https://doi.org/10.1016/j.measen.2023.100709.

[9] Glass, T., Ali, S., Parr, B., Potgieter, J., & Alam, F. IoT enabled low cost air quality sensor. In *2020 IEEE Sensors Applications Symposium (SAS).2020,* (pp. 1-6). IEEE. https://doi.org/10.1109/SAS48726.2020.9220079.

[10] Arroyo, P., Gómez-Suárez, J., Suárez, J.I. and Lozano, J. Low-cost air quality measurement system based on electrochemical and PM sensors with cloud connection. *Sensors*, 2021, *21*(18), p.6228. https://doi.org/10.3390/s21186228.

[11] Barot V, Kapadia V. Air quality monitoring systems using IoT: a review. In2020 international conference on computational performance evaluation (ComPE) 2020 Jul 2 (pp. 226-231). IEEE. https://doi.org/10.1109/ComPE49325.2020.9200053

[12] Kobbekaduwa, N., Oruthota, P., & De Mel, W. R. (2021). Calibration and implementation of heat cycle requirement of MQ-7 semiconductor

sensor for detection of carbon monoxide concentrations. https://doi.org/10.31357/AIT.V1I2.5068.
[13] MQ-135 GAS SENSOR. Available online: https://www.olimex.com/Products/Components/Sensors/SNS-MQ135/resources/SNS MQ135.pdf (accessed on 24 February 2025).
[14] WINSEN GAS SENSOR. Available online: Alldatasheet.com. *MQ135 Download*. https://www.alldatasheet.com/datasheet-pdf/download/1307647/WINSEN/MQ135.html (accessed on 24 February 2025).
[15] *Sensors*. (2021). Available online: https://pslab.io/sensors. (accessed on 24 February 2025).
[16] Idrees, Z., Zou, Z., & Zheng, L. (2018). Edge computing based IoT architecture for low cost air pollution monitoring systems: a comprehensive system analysis, design considerations & development. *Sensors*, *18*(9), 3021. https://doi.org/10.3390/s18093021.
[17] AirGradient (no date) *Shop*. Available at: https://www.airgradient.com/shop/ (Accessed 20 August 2025).
[18] IQAir (no date) *Home page*. Available at: https://www.iqair.com/(Accessed 20 August 2025).
[19] PurpleAir (no date) *Real-time air quality monitoring by PurpleAir*. Available at: https://www2.purpleair.com/(Accessed 20 August 2025).
[20] The World Air Quality Index project (no date) *GAIA A08 - Open Source Air Quality Monitor : compact & hackable air quality monitoring station*. Available at: https://aqicn.org/gaia/a08/(Accessed 20 August 2025).
[21] The World Air Quality Index project (no date b) *GAIA A12 Air Quality Monitoring Station*. Available at: https://aqicn.org/gaia/a12/(Accessed 20 August 2025).
[22] The World Air Quality Index project (no date c) *GAIA A18 Air Quality Monitoring Station: solar panel powered and long distance LoRA radio*. Available at: https://aqicn.org/gaia/a18/(Accessed 20 August 2025).
[23] Okafor, C. L., Chukwu, F. S., and Ahove, M. A. Comparative assessment of air quality in Epe, and Olusosun dumpsites of Nigeria. *Journal of Agriculture and Environmental Sciences*. 2024, *9*(1), 50-60. https://doi.org/10.4314/jaes.v9i1.4.
[24] Omokpariola, D.O., Nduka, J.N. and Omokpariola, P.L., 2024. Short-term trends of air quality and pollutant concentrations in Nigeria from 2018–2022 using tropospheric sentinel-5P and 3A/B satellite data. *Discover Applied Sciences*, *6*(4), p.182. https://doi.org/10.1007/s42452-024-05856-8.
[25] Owoade, O. K., Abiodun, P. O., Omokungbe, O. R., Fawole, O. G., Olise, F. S., Popoola, O. O., ... and Hopke, P. K. Spatial-temporal variation and local source identification of air pollutants in a semi-urban settlement in Nigeria using low-cost sensors. *Aerosol and Air Quality Research*. 2021, *21*(10), 200598. https://doi.org/10.4209/aaqr.200598.
[26] Mahmud, K., Mitra, B., Uddin, M. S., Hridoy, A. E. E., Aina, Y. A., Abubakar, I. R., ... and Rahman, M. M. Temporal assessment of air quality in major cities in Nigeria using satellite data. *Atmospheric Environment:* 2023, *20*, 100227. https://doi.org/10.1016/j.aeaoa.2023.100227.
[27] Daramola, S.O. and Makinde, E.O. Modeling air pollution around major dumpsites in Lagos State using geospatial methods with solutions. *Environmental Challenges*. 2024, *16*, p.100969. https://doi.org/10.1016/j.envc.2024.100969.
[28] Kumar, A., Sharma, G., Sharma, A., Chopra, P., and Rattan, P. (Eds.). Advances in Networks, Intelligence and Computing: Proceedings of the International Conference On Networks, Intelligence and Computing (ICONIC 2023) (1st ed.). CRC Press. https://doi.org/10.1201/9781003430421.
[29] Wegener, A. (1926). Thermodynamics of the atmosphere. In application of thermodynamics (pp. 156-189). Berlin, Heidelberg: Springer Berlin Heidelberg. https://doi.org/10.1007/978-3-642-90779-1_3.
[30] Harrell, J. W., and Gabler, M. C. (2023). The pressure point of altitude research. Journal of Applied Physiology, 135(5), 1213-1213. https://doi.org/10.1152/japplphysiol.00736.2023.
[31] Segun, A. A., Kehinde, D. A., and Adebmbo, A. A. (2018). Analysis of radio refractivity variations across geographical coordinates of Nigeria. Journal of Information Engineering and Applications, 8(3), 1-6.
[32] Okimiji, O. P., Techato, K., Simon, J. N., Tope-Ajayi, O. O., Okafor, A. T., Aborisade, M. A., and Phoungthong, K.. Spatial pattern of air pollutant concentrations and their relationship with meteorological parameters in coastal slum settlements of Lagos, Southwestern Nigeria. *Atmosphere*. 2021, *12*(11), 1426. https://doi.org/10.3390/atmos12111426.
[33] Yang, Y., Fan, S., Wang, L., Gao, Z., Zhang, Y., Zou, H., ... and Lolli, S. Diurnal evolution of the wintertime boundary layer in urban Beijing, China: Insights from Doppler Lidar and a 325-m meteorological tower. *Remote Sensing*. 2020, *12*(23), 3935. https://doi.org/10.3390/rs12233935.
[34] Askariyeh, M.H., Vallamsundar, S. and Farzaneh, R. Investigating the impact of meteorological conditions on near-road pollutant dispersion between daytime and nighttime periods. *Transportation Research Record*. 2018, *2672*(25), pp.99-110. https://doi.org/10.1177/0361198118796966.
[35] Jbara, A. A. Environmental and Health Impacts Resulting From Burning Solid Waste Near Residential Areas in Diyala Governorate, Iraq. *Academia Open*. 2024, *9*(2), 10-21070. https://doi.org/10.21070/acopen.9.2024.10088.
[36] Hart, R., Liang, L., and Dong, P. Monitoring, mapping, and modeling spatial–temporal patterns of PM2. 5 for improved understanding of air pollution dynamics using portable sensing technologies. *International journal of environmental research and public health*. 2020, *17*(14), 4914. https://doi.org/10.3390/ijerph17144914.
[37] Arunab, K.S. and Mathew, A. Quantifying urban heat island and pollutant nexus: A novel geospatial approach. *Sustainable Cities and Society*. 2024, *101*, p.105117. https://doi.org/10.1016/j.scs.2023.105117.
[38] Vanaja M, D. P., Esakkiammal A, Parameshwari M. V, M. Afrinaa, and Thangaraj J. Air Quality Monitoring System Using Arduino. In 2025 *International Conference on Advanced Computing Technologies (ICoACT)*, Sivalasi, India. 2025, (pp. 1-6). IEEE. https://doi.org/10.1109/ICoACT63339.2025.11005322.
[39] Aceveda, E.J.B., Lopez, E.S., Mendoza, C.D.H., Delmo, J.A.B., Sarmiento, J.S. and Rayos, M.J.F.T. Evaluating the Correlation between MQ Gas Sensors with Temperature and Humidity Sensor on an Outdoor Setting. In *2024 14th International Conference on System Engineering and Technology (ICSET)*. 2024, (pp. 12-16). IEEE. https://doi.org/10.1109/ICSET63729.2024.10774817
[40] Mishra, G., Sharma, A., Shaini, A., and Saxena, S. Air Quality Monitoring Using MQ135 Gas Sensor and Arduino Uno. *International Journal of Latest Technology in Engineering, Management & Applied Science*. 2025, *14*(5), 1097-1101. https://doi.org/10.51583/ijltemas.2025.140500119.
[41] Tariq, H., Abdaoui, A., Touati, F., Al-Hitmi, M. A. E., Crescini, D., and Manouer, A. B. A real-time gradient aware multi-variable handheld urban scale air quality mapping IoT system. In *2020 IEEE International Conference on Design & Test of Integrated Micro & Nano-Systems (DTS). 2020,* (pp. 1-5). IEEE.
[42] Vannucci, P. F., and Cohen, R. C. Temperature-Dependent Nighttime Stagnation Episodes Driving Decadal Air Pollutant Exceedances in Los Angeles. *ACS ES&T Air*. 2024, *1*(6), 474-480. https://doi.org/10.1021/acsestair.3c00080.
[43] Levy, I., Mihele, C., Lu, G., Narayan, J., and Brook, J. R. Evaluating multipollutant exposure and urban air quality: pollutant interrelationships, neighborhood variability, and nitrogen dioxide as a proxy pollutant. *Environmental health perspectives*. 2014, *122*(1), 65-72. https://doi.org/10.1289/ehp.1306518.
[44] Zhang, H., Wang, Y., Hu, J., Ying, Q.,and Hu, X. M. Relationships between meteorological parameters and criteria air pollutants in three megacities in China. *Environmental research*. 2015, *140*, 242-254. https://doi.org/10.1016/j.envres.2015.04.004.
[45] Wei, C., Wang, M., Fu, Q., Dai, C., Huang, R., & Bao, Q. (2020). Temporal characteristics of greenhouse gases ($CO_2$ and $CH_4$) in the megacity Shanghai, China: Association with air pollutants and meteorological conditions. *Atmospheric Research*, *235*, 104759. https://doi.org/10.1016/j.atmosres.2019.104759
[46] Fikeraddis, M. and Endeshaw, L. Influence of temperature and relative humidity on air pollution in Addis Ababa, Ethiopia. *Journal of Environmental & Earth Sciences. 2020*, *2*(2). https://doi.org/10.30564/jees.v2i2.2286.
[47] Ulutaş, K., Abujayyab, S. K., and Amr, S. A., 2021. Evaluation of the major air pollutants levels and its interactions with meteorological parameters in Ankara. *Mühendislik Bilimleri ve Tasarım Dergisi*, *9*(4), 1284-1295. https://doi.org/10.21923/jesd.939724.
[48] Lelandais, L., Xueref-Remy, I., Riandet, A., Blanc, P. E., Armengaud, A., Oppo, S., ... and Delmotte, M. Analysis of 5.5 years of atmospheric CO2, CH4, CO continuous observations (2014–2020) and their correlations, at the Observatoire de Haute Provence, a station of the ICOS-France national greenhouse gases observation network. *Atmospheric Environment*. 2022, *277*, 119020. https://doi.org/10.1016/j.atmosenv.2022.119020.
[49] Qi, X., Mei, G., Cuomo, S., Liu, C., and Xu, N. Data analysis and mining of the correlations between meteorological conditions and air quality: A case study in Beijing. *Internet of Things*. 2021, *14*, 100127. https://doi.org/10.1016/j.iot.2019.100127.
[50] Tope, A. T., Sawyerr, H. O., and Afolabi, O. O. Dumpsite Emissions in Southwestern Nigeria: Assessing the Relationships Between Atmospheric Conditions, Ghgs and Air Pollutant. *International Journal of Latest Technology in Engineering, Management & Applied Science*. 2025, *14*(5), 1013-1017. https://doi.org/10.51583/ijltemas.2025.140500106.
[51] Owoade, O. K., Abiodun, P. O., Omokungbe, O. R., Fawole, O. G., Olise, F. S., Popoola, O. O., ... & Hopke, P. K. (2021). Spatial-temporal variation and local source identification of air pollutants in a semi-urban settlement in Nigeria using low-cost sensors. *Aerosol and Air Quality Research*, *21*(10), 200598. https://doi.org/10.4209/aaqr.200598.
[52] Whitehill, A. R., Long, R. W., Urbanski, S. P., Colón, M., Habel, A., & Landis, M. S. (2022). Evaluation of Cairpol and Aeroqual air sensors in biomass burning plumes. *Atmosphere*, *13*(6), 877. https://doi.org/10.3390/atmos13060877.
[53] Martin, C. R., Zeng, N., Karion, A., Dickerson, R. R., Ren, X., Turpie, B. N., & Weber, K. J. (2017). Evaluation and environmental correction of

ambient $CO_2$ measurements from a low-cost NDIR sensor. *Atmospheric measurement techniques*, *10*(7), 2383-2395. https://doi.org/10.5194/AMT-10-2383-2017.

[54] Bauerová, P., Šindelářová, A., Rychlík, Š., Novák, Z., & Keder, J. (2020). Low-Cost Air Quality Sensors: One-Year Field Comparative Measurement of Different Gas Sensors and Particle Counters with Reference Monitors at Tušimice Observatory. *Atmosphere*, *11*(5), 492. https://doi.org/10.3390/atmos11050492.

[55] Diez, S., Lacy, S., Coe, H., Urquiza, J., Priestman, M., Flynn, M., ... & Edwards, P. M. (2024). Long-term evaluation of commercial air quality sensors: an overview from the QUANT (Quantification of Utility of Atmospheric Network Technologies) study. *Atmospheric Measurement Techniques*, *17*(12), 3809-3827. https://doi.org/10.5194/amt-17-3809-2024.

[56] Dheer, I., Mehta, S., Somanchi, S., Nelson, A., & Srivastava, A. (2025). Pre-Deployment Calibration Framework for Low-Cost Gas Sensors: An Adaptive Environmental Parameter Model. IEEE Sensors Letters. https://doi.org/10.1109/LSENS.2025.3576152.

[57] Buehler, C., Xiong, F., Zamora, M. L., Skog, K. M., Kohrman-Glaser, J., Colton, S., ... & Gentner, D. R. (2021). Stationary and portable multipollutant monitors for high-spatiotemporal-resolution air quality studies including online calibration. *Atmospheric measurement techniques*, *14*(2), 995-1013. https://doi.org/10.5194/amt-14-995-2021.

[58] Araújo, T., Silva, L., & Moreira, A. (2020). Evaluation of low-cost sensors for weather and carbon dioxide monitoring in internet of things context. *IoT*, *1*(2), 286-308. https://doi.org/10.3390/iot1020017.